Spin dependence of critical point behavior for first and second order phase transitions in nuclei

E. Williams, R. J. Casperson, and V. Werner

A.W. Wright Nuclear Structure Laboratory, Yale University, New Haven, Connecticut 06520, USA

A study of first and second order nuclear shape phase transitional behavior in yrast states of even-even nuclei in the context of the Interacting Boson Model-1 is presented. Finite boson number effects are identified using calculations with up to 150 bosons, and the role of the rotational degree of freedom of observables in first and second order quantum phase transitional nuclei is discussed. We aim to provide a first investigation of the angular momentum dependence of experimentally accessible phase transitional signatures in finite-sized quantum nuclear systems.

Quantum phase transitions (QPTs) are a subject of intense interest in many areas of physics, as such transitional phenomena play important roles in everything from atomic nuclei [1–6] to quantum Hall systems [7,8]. Second order QPTs have been the primary focus of research, as Landau's classical theory of continuous phase transitions can be simply extended to quantum systems exhibiting such behavior [9,10].

First order QPTs, on the other hand, cannot be viewed as an easy extension of well-explored continuous (classical) models. Theoretical approaches for defining and understanding the complexities of such behavior have not yet been developed, and even basic questions about experimental signatures of first order QPT behavior remain unanswered. As such, not much progress has been made in identifying the measurable differences between these two transition types in finite systems—particularly concerning the existence of excited state QPTs [11] in both orders, which are the focus of this work. Pinpointing such observable distinctions between first and second order QPT behavior is an essential first step in making progress on testing currently available models of such systems and in developing a more complete theory of QPTs.

The atomic nucleus is an ideal system for probing first and second order QPT behavior in a finite system. First and second order quantum shape phase transitions in nuclei were first identified in a theoretical framework in 1980, when the coherent state formalism [12–14] was used to derive a potential energy surface (and thus, a picture of something like the free energy surface) [1,15] within the context of the Interacting Boson Model-1 (IBM-1) [16]. More recent work has explored geometric models (see, e.g., Refs. [3,5,17–20]), the IBM-1 [21–27], and experimental examples of possibly phase transitional nuclei [26,28–31]. A more direct connection to Landau's classical theory has also been proposed, in the form of a phase diagram for nuclear structure, akin to that of water [10]. A similar approach to the problem has been constructed in terms of nuclear pairing properties [32]. All of this work has fueled the construction of a theoretical framework and a search for experimental evidence of such QPT behavior in this naturally occurring two-component condensed matter system.

In nuclei, much of the recent work on second order QPTs [4,6,10,33–37] has made use of the IBM-1. The model offers a means of studying the evolution of low-lying collective states via a simple, two-parameter, Ising-type Hamiltonian and is useful for identifying finite size effects on phase transitional signatures in many different types of quantum bosonic systems [37].

In the IBM-1, finite boson (N) effects smooth out the evolution of all observables of a given system. This smoothing becomes less prevalent as system size is increased, so distinctions between gradual evolutionary trajectories of system observables and signatures of QPT behavior, which, by definition, exhibit discontinuities in the continuous limit, can only be made by exploring the system's behavior as a function of N over a large range of system sizes.

Thus far, most of the work on QPTs in nuclei has focused on the behavior of the energies of states with seniority 0 near the second order phase transition (e.g., Refs. [11,33,38]). Beyond this, Rowe and Rosensteel have previously examined the behavior of both ground and excited state observables in large ($N \leqslant 100$) finite boson systems near both first and second order QPTs in the IBM-1 [39–41]. Their use of the quasidynamical symmetry concept to classify vibrator- or rotor-like behavior in the first order case, which they support with calculations of energies, transition strength ratios, and wave functions for finite-boson systems, provides an important foundation for further studies of first order QPTs in the IBM-1. Additional work by Rowe, Turner, and Rosensteel [35] has explored the asymptotic behavior of excitation energies with increasing system size at both the first and second order critical points. Cejnar [42,43] has also investigated the role angular momentum plays in the geometric behavior of both the first and second order QPT system in a mean field study performed in the coherent state formalism [12–14] using IBM-1 with cranking.

The present work explicitly investigates the role angular momentum plays in the evolution of excited state QPT behavior in finite systems. Our approach assumes nothing more than the presence of either a first or a second order phase transition in the ground state of an equivalent infinite N system. In contrast to Ref. [35], we do not study the behavior of observables at the infinite size critical point; instead, we observe the evolution of energies and transition strengths with respect to angular momentum over a wide range of boson numbers ($10 \leqslant N \leqslant 150$), between pairs of symmetry limits in the IBM-1. We aim to (1) identify whether angular momentum plays a role in QPT behavior in the finite

size limit and (2) determine how to associate properties of QPT behavior in the large N limit with observable trends in experimentally accessible, finite N systems. To address these points, numerical studies of the first and second order QPTs approaching the large N limit of the IBM-1 are presented. The yrast states up to spin 20 are examined across both transitions.

All calculations in this work utilized a simple, two-parameter version of the IBM-1 Hamiltonian [44,45], which invokes the Extended [46] Consistent Q Formalism [47]:

$$H_{\text{ECQF}}(\zeta) = c \left[(1 - \zeta)n_d - \frac{\zeta}{4N} Q^\chi \cdot Q^\chi \right], \quad (1)$$

where N is the boson number, c is a scaling factor, $n_d = d^\dagger \cdot \tilde{d}$ is the d-boson number operator, and Q^χ, given by $Q^\chi = [d^\dagger \tilde{s} + s^\dagger \tilde{d}]^{(2)} + \chi [d^\dagger \tilde{d}]^{(2)}$, is the quadrupole operator. The $E2$ transition operator is defined as

$$T(E2) = e_B Q^\chi, \quad (2)$$

where e_B is the effective boson charge. In all numerical calculations in this work, $e_B = 1$ and $c = 1$.

In this parametrization, U(5) (vibrational structure) corresponds to $\zeta = 0$, all χ; SU(3) (axially symmetric rotational structure) corresponds to $\zeta = 1$, $\chi = -\sqrt{7}/2$; and O(6) (soft, axially asymmetric rotational structure) corresponds to $\zeta = 1$, $\chi = 0$. A first order transition occurs for $\chi = -\sqrt{7}/2$, between the U(5) and SU(3) limits, whereas a second order transition occurs for $\chi = 0$, between the U(5) and O(6) limits [1].

Studies of critical point behavior depend on the identification of an order parameter. An order parameter is an observable (derivative of an observable with respect to the control parameter) that exhibits discontinuous behavior at the critical point of a first (second) order phase transition. One option is $\partial E(0_1^+)/\partial \zeta \equiv \nu(0_1^+)$, the derivative of the energy of the ground state with respect to the control parameter, ζ, as it is proportional to a quantity akin to the "specific heat" of this quantum system [36]. $E(0_1^+)$ is not the binding energy; it corresponds to the decrease in energy of a given state due to an increase in the system's deformation. In classical systems, discontinuities in the specific heat (or its derivatives) have been used to investigate properties of a system exhibiting QPT behavior. As such, we will use $\nu(0_1^+)$ as an order parameter, but will extend this idea to excited yrast states with spin J. $\nu(J_1^+)$ will be one order parameter of interest.

To draw a more direct comparison to geometric descriptions, observables that relate more directly to deformation parameters β and γ—or their average values, as they are not rigid in general—are useful. Quadrupole shape invariants [48,49] fulfill this requirement [44] and are more broadly applicable than β and γ, because they are model-independent observables.

For brevity, we restrict our discussion of shape invariants to $q_2(J_1^+)$, which is defined in terms of the quadrupole transition operator $T(E2)$. In accordance with Eq. (2), $q_2(J)$ is given as follows [44]:

$$q_2(J) = |\langle J | Q^\chi \cdot Q^\chi | J \rangle|. \quad (3)$$

The quantity $q_2(J)$ is proportional to $\langle J | \beta^2 | J \rangle$; the proportionality constant depends only on the charge and radius of the nucleus. Therefore, we treat $q_2(J_1^+)$ as an alternate order parameter in this work.

Calculations across transitional regions U(5)-SU(3) and U(5)-O(6) have been performed using the new IBM-1 code IBAR [50], for a large range of boson numbers ($10 \leqslant N \leqslant 150$, in steps of 10), to study the differences between first and second order phase transitional behavior in nuclei. IBAR was developed to provide the high precision demanded by the rapid evolution of various observables near the critical point. The current study is restricted to the yrast states, up to spin 20. For each N, over 100 calculations were carried out from $\zeta = 0$ to $\zeta = 1$. Smaller steps were taken near the phase transition to ensure an adequate reproduction of the critical point behavior.

Finding a numerical means of extracting the critical point was necessary to study the evolution of the critical point with increasing J and N. Following the procedure given in Ref. [27], we defined the "effective" critical point, ζ_c, as the point at which the change in the order parameter (derivative of the order parameter) is most rapid for a finite N calculation at the first (second) order transition. This value approximately corresponds to the point at which the order parameter or its derivative becomes discontinuous in the infinite N limit, and, as defined, mirrors the typical experimental procedure used to identify QPT behavior in isotopic/isotonic chains.

To determine the value of ζ_c, spline functions were fit to the calculated observables of interest and were then differentiated once, twice, or three times (for energies only), depending on the order of phase transition. For the second order case, the Lanczos algorithm used to facilitate higher boson calculations produced occasional fluctuations in q_2, which we attribute to the underlying O(5) symmetry along the U(5)-O(6) transition. In these cases, we compared results to those obtained with a full diagonalization of the Hamiltonian to ensure the accuracy of our results, where possible, and graphically confirmed the location of the extremum of the second derivative of $q_2(J_1^+)$ for each set of calculations. The numerical error introduced in our methods was $<1\%$ for the energies and $<5\%$ for the shape invariants.

A comparison between the ground state energies along both the U(5)-SU(3) (first order) and U(5)-O(6) (second order) transitions, as shown in Figs. 1(a) and 1(b), respectively, illustrates the distinctive behavior exhibited by such observables depending on the type of phase transition. Along U(5)-SU(3), the deviation from zero for all N increases sharply and rapidly in the vicinity of the critical point. In contrast, along U(5)-O(6), the deviation from zero near the critical point for all boson numbers varies smoothly and slowly with increasing ζ.

Examining the relevant derivatives of the ground state energies with respect to ζ further highlights the distinction between the two transition types. For U(5)-SU(3), the order parameter $\nu(0_1^+)$ becomes increasingly step function-like as N increases, as shown in Fig. 1(c). Taking the derivative once again [Fig. 1(e)] highlights the increasingly discontinuous behavior of the order parameter with increasing N.

At the U(5)-O(6) transition, a discontinuity in the derivative of the order parameter is expected. This is illustrated in the plot of $\partial \nu(0_1^+)/\partial \zeta$ in Fig. 1(d), which is similar in shape but far smoother and smaller in overall magnitude at its minimum than the same quantity [Fig. 1(e)] along U(5)-SU(3). In Fig. 1(f),
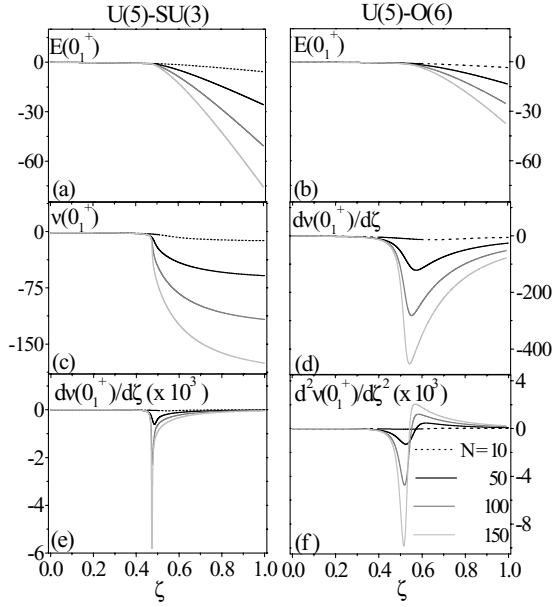
FIG. 1. The unnormalized energies for (a) U(5)-SU(3) and (b) U(5)-O(6); cases are plotted for $N = 10, 50, 100, 150$. (c) $\nu(0_1^+)$ for U(5)-SU(3) and (d) $\partial \nu(0_1^+)/\partial \zeta$ for U(5)-O(6) are plotted. Finally, (e) $\partial \nu(0_1^+)/\partial \zeta$ for U(5)-SU(3) and (f) $\partial^2 \nu(0_1^+)/\partial \zeta^2$ for U(5)-O(6), from which $\zeta_c(0_1^+)$ is extracted, are shown. For higher J states, the behavior of the energies and their subsequent derivatives is similar, though boson saturation effects are more evident.

one can confirm that the second order treatment for U(5)-O(6) is valid by observing that $|\partial^2 \nu(0_1^+)/\partial \zeta^2|$ approaches infinity with increasing N. The extrema of the derivatives of the relevant discontinuous quantities, whose ζ values correspond to the effective critical point ζ_c, are of the same order of magnitude for both U(5)-SU(3) and U(5)-O(6) [Figs. 1(e) and 1(f)].

In Fig. 2, $\zeta_c(J_1^+)$ for several N, as extracted from $\nu(J_1^+)$, is shown for both U(5)-SU(3) and U(5)-O(6). In the first order case, ζ_c occurs at smaller ζ values for higher J in low N cases, as shown in Fig. 2(c) for the example of $N = 10$.
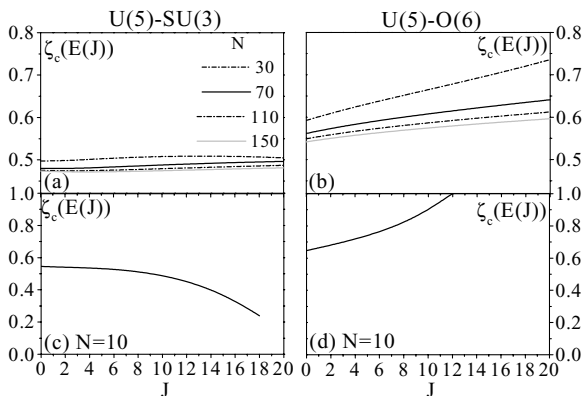

FIG. 2. $\zeta_c(J)$, as determined from the energy calculations, is shown for (a) U(5)-SU(3), $N = 30, 70, 110, 150$; (b) U(5)-O(6), $N = 30, 70, 110, 150$; (c) U(5)-SU(3), $N = 10$; and (d) U(5)-O(6), $N = 10$.
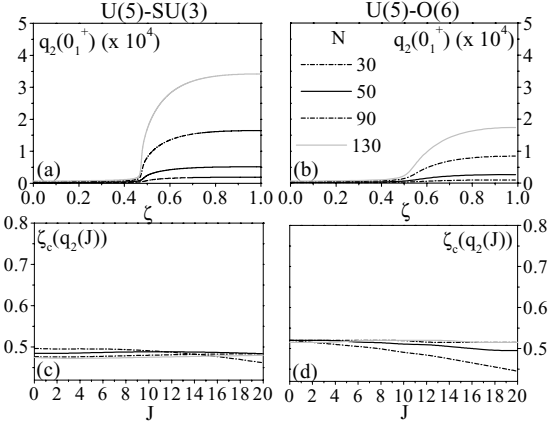

FIG. 3. In the upper panels, a plot of $q_2(0_1^+)$ with respect to ζ is shown for (a) U(5)-SU(3) and (b) U(5)-O(6) for $N = 30, 50, 90, 130$. In the lower panels, the spin dependence of $\zeta_c(J_1^+)$ extracted from $q_2(J)$ for $N = 30, 50, 90, 130$ is shown for (c) U(5)-SU(3) and (d) U(5)-O(6).

In this case, finite N effects are prevalent, especially in the dramatic decrease in $\zeta_c(J_1^+)$ for high J. This effect appears for J approaching $2N$ in large N cases as well and is a result of the fact that the IBM system scales with N. For higher N calculations, plotted in Fig. 2(a), $\zeta_c(J_1^+)$ becomes increasingly flat with increasing N and converges to the ground state coherent state result in the infinite N limit ($\zeta_c = 8/17$) [51]. In the second order case, the opposite behavior with respect to spin for lower N is evident in Fig. 2(d); $\zeta_c(J_1^+)$ increases with increasing spin for lower N. Again, convergence toward the ground state coherent state result ($\zeta_c = 1/2$) is suggested from Fig. 2(b), but is much slower for this transition. Because of the current N limit of our code, convergence can only be surmised.

When using $q_2(J_1^+)$ as the order parameter, however, the evolution of QPT behavior takes an alternate path. For reference, plots of $q_2(0_1^+)$ are shown in Figs. 3(a) and 3(b) for several N and both U(5)-SU(3) and U(5)-O(6). $\zeta_c(J_1^+)$ extracted from q_2 for multiple N is shown in Figs. 3(c) and 3(d). In both the first and second order cases, ζ_c occurs at lower values of ζ with increasing J for small N. Again, this effect is tempered in higher N calculations, and convergence toward the coherent state critical points ($\zeta = 8/17$ for first order, $\zeta = 1/2$ for second order) is evident.

Interestingly, the evolution of ζ_c as derived from either $\nu(J_1^+)$ or $q_2(J_1^+)$ is consistent with Cejnar's finding [42,43] for the U(5)-SU(3) leg. If one compares Fig. 1 in Ref. [43] to Fig. 2(c) in this work (keeping in mind that $\eta = 1$ corresponds to the U(5) limit in Cejnar's parametrization), it is clear that both methods predict that the critical point will head toward U(5) with increasing angular momentum. The same holds true for low N calculations with $q_2(J_1^+)$ along U(5)-O(6).

In contrast, the ζ_c values extracted from $\nu(J_1^+)$ between U(5)-O(6) contradict Cejnar's result, which predicts the same critical point evolution with angular momentum for both U(5)-SU(3) and U(5)-O(6) in the infinite boson limit. However, the two models differ significantly, as the present work introduces no cranking and is specifically focused on finite N systems,

whereas Refs. [42] and [43] explore similar questions with cranking, using an energy potential surface derived with the coherent state formalism for the infinite N case. Also, the critical point line in Fig. 1 of Ref. [43] actually represents a separatrix between two phases. In the present work, the $\zeta_c(J_1^+)$ lines cannot be interpreted in the same way, because the wave functions exhibit mixed character [both U(5) and SU(3) or O(6) components] on either side of the critical point [41]. ζ_c is simply the point of greatest change in the order parameter (or its derivative), as this is generally used to identify the critical point in experimental work. Our work shows that ζ_c actually evolves into the infinite N critical point of a complementary continuous QPT system.

One may note that our results for higher N converge to one value, rather than maintain a characteristic J-dependent trajectory. This is surprising at first, because such large N systems should converge to the infinite N coherent state-based critical behavior discussed in Refs. [42] and [43]. However, our calculations were limited to $J \leqslant 20$ to follow the trajectory of states with specific quantum numbers as a function of N. As Cejnar [43] illustrates in Fig. 6, $J = N$ is close to the maximum spin at which the U(5)-SU(3) phase transition is still evident for finite systems.

The order parameter's effect on the evolution of ζ_c behavior for the second order case gives rise to the question of the role observable-dependent finite size effects play on such studies. As Dusuel et al. [37] found, scaling behavior of different observables in a given system, as defined by the asymptotic behavior of each observable at the critical point in the infinite N limit, differs depending on the observable in question. In the second order case, the $B(E2; 0_1^+ \rightarrow 2_1^+)$ value scales as $+4/3$; this is quite different from the scaling behavior of the energy gap between the two states $[E(2_1^+) - E(0_1^+)]$, which goes as $-1/3$ [37]. Such quantitative differences in the scaling behavior of system observables at the infinite N critical point will be reflected in the opposing evolution of ζ_c with increasing J. As such, one must note that observables used to examine QPT behavior in nuclei may not exhibit identical finite size effects. In turn, one must not expect to find QPT behavior (in terms of a rapid change in system observables) for all states or observables in a single nucleus. QPT signatures will instead be found in different states in a given nucleus and even across different members of an isotopic/isotonic chain.

Nevertheless, ζ_c behavior in the yrast band is sensitive to the angular momentum of the state in question, as shown in Figs. 2 and 3. In the case of $\nu(J_1^+)$ for low N, the distinctive evolution of ζ_c for the first and second order transitions for small N systems is intriguing, as $N \sim 10$ corresponds to the typical size of existing nuclear systems ($N \leqslant 16$). As such, these differences may be detectable in isotopic chains accessible to experiment. In an investigation of the yrast energies of rare earth nuclei by Zhang [52], ζ_c was identified as the inflection point of backbending in gauge space. While this description is outside of the scope of the calculations presented here, as absolute binding energies are not calculated with the Hamiltonian given in Eq. (1), one can compare the results on an interpretive basis. In comparing Figs. 2 and 4 in Ref. [52] and Fig. 2(c) herein, it becomes evident that both works—despite different approaches—show the same result: that ζ_c occurs for lower values of ζ for the first order case. Note that the neutron number N in Ref. [52] is analogous to the control parameter ζ used in this work. For the second order case, the current data available in isotopic chains including such transitional nuclei (e.g., ^{134}Ba [28]) are insufficient to perform a similar analysis, though E-GOS methods presented by Regan et al. [53] may help shed some light on the J dependence of critical point behavior in these nuclei.

This novel investigation has established that critical point behavior in finite nuclear systems varies smoothly with respect to angular momentum. This point is important from an experimental perspective, as it establishes the possibility that QPT behavior in nuclei occurs in different members of isotopic/isotonic chains for states of different angular momentum. In addition, this work has found that the explicit role angular momentum plays in effective critical point behavior in finite systems depends on both the choice of order parameter and on the order of the QPT. The observed convergence to the same critical point for all higher angular momentum states using either order parameter in the large N limit provides evidence of the presence of real first and second order QPTs for excited yrast states in the infinite boson limit.

[1] A. E. L. Dieperink, O. Scholten, and F. Iachello, Phys. Rev. Lett. **44**, 1747 (1980); A. E. L. Dieperink and O. Scholten, Nucl. Phys. **A346**, 125 (1980).
[2] R. F. Casten, Dimitri Kusnezov, and N. V. Zamfir, Phys. Rev. Lett. **82**, 5000 (1999).
[3] F. Iachello, Phys. Rev. Lett. **85**, 3580 (2000).
[4] P. Cejnar and J. Jolie, Phys. Rev. E **61**, 6237 (2000).
[5] F. Iachello, Phys. Rev. Lett. **87**, 052502 (2001).
[6] P. Cejnar, M. Macek, S. Heinze, J. Jolie, and J. Dobeš, J. Phys. A **39**, L515 (2006).
[7] B. Huckestein, Rev. Mod. Phys. **67**, 357 (1995).
[8] S. L. Sondhi, S. M. Girvin, J. P. Carini, and D. Shahar, Rev. Mod. Phys. **69**, 315 (1997).
[9] S. Sachdev, *Quantum Phase Transitions* (Cambridge University Press, Cambridge, UK, 1999).
[10] J. Jolie, P. Cejnar, R. F. Casten, S. Heinze, A. Linnemann, and V. Werner, Phys. Rev. Lett. **89**, 182502 (2002).
[11] M. A. Caprio, P. Cejnar, and F. Iachello, Ann. Phys. **323**, 1106 (2008).
[12] R. Gilmore, C. M. Bowden, and L. M. Narducci, Phys. Rev. A **12**, 1019 (1975).
[13] R. Gilmore and D. H. Feng, Phys. Lett. **B76**, 26 (1978).
[14] R. Gilmore and D. H. Feng, Nucl. Phys. **A301**, 189 (1978).
[15] J. N. Ginocchio and M. W. Kirson, Nucl. Phys. **A350**, 31 (1980).
[16] F. Iachello and A. Arima, *The Interacting Boson Model* (Cambridge University Press, Cambridge, UK, 1987).

[17] Dennis Bonatsos, D. Lenis, N. Minkov, P. P. Raychev, and P. A. Terziev, Phys. Rev. C **69**, 014302 (2004).

[18] Lorenzo Fortunato, Phys. Rev. C **70**, 011302(R) (2004).

[19] N. Pietralla and O. M. Gorbachenko, Phys. Rev. C **70**, 011304(R) (2004).

[20] Dennis Bonatsos, D. Lenis, D. Petrellis, P. A. Terziev, and I. Yigitoglu, Phys. Lett. **B632**, 238 (2006).

[21] O. Castaños, A. Frank, and P. Federman Phys. Lett. **B88**, 203 (1979).

[22] E. López-Moreno and O. Castaños Phys. Rev. C **54**, 2374 (1996).

[23] J. Jolie, P. Cejnar, and J. Dobeš, Phys. Rev. C **60**, 061303R (1999).

[24] J. M. Arias, C. E. Alonso, A. Vitturi, J. E. García-Ramos, J. Dukelsky, and A. Frank, Phys. Rev. C **68**, 041302R (2003).

[25] J. E. García-Ramos, J. Dukelsky, and J. M. Arias, Phys. Rev. C **72**, 037301 (2005).

[26] E. A. McCutchan, N. V. Zamfir, and R. F. Casten, Phys. Rev. C **71**, 034309 (2005).

[27] V. Werner, P. von Brentano, R. F. Casten, and J. Jolie, Phys. Lett. **B527**, 55 (2002).

[28] R. F. Casten and N. V. Zamfir, Phys. Rev. Lett. **85**, 3584 (2000).

[29] R. F. Casten and N. V. Zamfir, Phys. Rev. Lett. **87** 052503 (2001).

[30] R. Krücken *et al.*, Phys. Rev. Lett. **88**, 232501 (2002).

[31] D. Tonev *et al.* Phys. Rev. C **69**, 034334 (2004).

[32] R. M. Clark, A. O. Macchiavelli, L. Fortunato, and R. Krücken, Nucl. Phys. **A787**, 524 (2007).

[33] P. Cejnar, S. Heinze, and J. Jolie, Phys. Rev. C **68**, 034326 (2003).

[34] F. Iachello and N. V. Zamfir, Phys. Rev. Lett. **92**, 212501 (2004).

[35] D. J. Rowe, P. S. Turner, and G. Rosensteel, Phys. Rev. Lett. **93**, 232502 (2004).

[36] P. Cejnar, S. Heinze, and J. Dobeš, Phys. Rev. C **71**, 011304R (2005).

[37] S. Dusuel, J. Vidal, J. M. Arias, J. Dukelsky, and J. E. García-Ramos, Phys. Rev. C **72**, 064332 (2005).

[38] D. A. Meyer *et al.*, Phys. Lett. **B638**, 44 (2006).

[39] D. J. Rowe, Phys. Rev. Lett. **93**, 122502 (2004).

[40] D. J. Rowe, Nucl. Phys. **A745**, 47 (2004).

[41] G. Rosensteel and D. J. Rowe, Nucl. Phys. **A759**, 92 (2005).

[42] P. Cejnar, Phys. Rev. C **65**, 044312 (2002).

[43] P. Cejnar, Phys. Rev. Lett. **90**, 112501 (2003).

[44] V. Werner, N. Pietralla, P. von Brentano, R. F. Casten, and R. V. Jolos, Phys. Rev. C **61**, 021301R (2000).

[45] N. V. Zamfir, P. von Brentano, R. F. Casten, and J. Jolie, Phys. Rev. C **66**, 021304(R) (2002).

[46] P. O. Lipas, P. Toivonen, and D. D. Warner, Phys. Lett. **B155**, 295 (1985).

[47] D. D. Warner and R. F. Casten, Phys. Rev. Lett. **48**, 1385 (1982).

[48] K. Kumar, Phys. Rev. Lett. **28**, 249 (1972).

[49] D. Cline, Annu. Rev. Nucl. Part. Sci. **36**, 683 (1986).

[50] R. J. Casperson, IBAR (Yale University, unpublished), 2006.

[51] N. V. Zamfir and G. E. Fernandes, in *Proceedings of the Eleventh International Symposium on Capture γ-Ray Spectroscopy and Related Topics*, edited by J. Kvasil, P. Cejnar, and M. Krticka (World Scientific, Singapore, 2003).

[52] J. Y. Zhang, Nucl. Phys. **A421**, 353c (1984).

[53] P. H. Regan *et al.* Phys. Rev. Lett. **90**, 152502 (2003).